Placenta 175 (2026) 25–32

Contents lists available at ScienceDirect

Placenta

journal homepage: www.elsevier.com/locate/placenta

Structural alterations in the placental villous tree in well-controlled gestational diabetes mellitus

N. Barapatre [a,*], L. Halm [a], C. Schmitz [a], F.E. von Koch [b], C. Kampfer [a], H-G. Frank [a]

[a] LMU Munich, Department of Anatomy II, Pettenkoferstr. 11, Munich, 80336, Germany
[b] Clinic for Obstetrics and Gynecology, Dritter Orden, Menzinger Str. 44, Munich, 80638, Germany

ARTICLE INFO

Keywords:
Gestational diabetes
Placenta
Trophoblast turnover
Villous tree
Stereology
3D microscopy

ABSTRACT

Introduction: A poorly controlled gestational diabetes mellitus (GDM), a metabolic disorder affecting glucose regulation, can lead to macrosomia in both, the placenta and the fetus. A well-managed GDM usually results in an uncomplicated pregnancy. Though some qualitative histopathological changes have been described in such uncomplicated pregnancies, a quantitative description of the structural alterations is still missing. The aim of this study is to assess the villous trophoblast and the villous tree quantitatively in GDM placentas, stratified according to the fetal sex.

Methods: The villous trees from 20 placentas (10 female and 10 male) affected by GDM and 20 Control placentas (10 female and 10 male) were investigated quantitatively by Stereology and 3D microscopy. The measurement of partial volumes of contractile and non-contractile parts of the villous tree was based on immunohistochemical detection of perivascular myofibroblasts. The villous trophoblast was assessed by 3D microscopy to measure the nuclear surface density.

Results: Only the female GDM placentas show an increase in the density of proliferative trophoblast nuclei and a decrease in the density of non-proliferative trophoblast nuclei. The branching index is reduced in GDM placentas irrespective of the sex. No significant difference was observed in the volumes of the villous tree, the intervillous space, and the fetal vessels. Similarly, the diffusion distance remained unchanged.

Conclusion: Even in well-controlled GDM pregnancies, the villous trophoblast shows a sexually dimorphic alteration in the density of proliferative and non-proliferative nuclei. The branching index, however, is reduced for both villous compartments, independent of fetal sex.

1. Introduction

The human placenta facilitates the transfer of nutrients, removal of waste, and gas exchange between the mother and fetus [1]. Beyond these functions, it plays a critical role in regulating and maintaining pregnancy by producing hormones such as progesterone and human chorionic gonadotropin [1]. The placenta balances and mediates maternal and fetal metabolic and endocrine environments, but disruptions in these systems can alter placental structure and function or result from these changes. One such disruption is maternal diabetes mellitus, a metabolic disorder affecting glucose regulation, which impacts placental structure and function [2–4]. Diabetes can develop during pregnancy (gestational diabetes mellitus, GDM) or exist prior to pregnancy (DM). Poorly controlled DM or GDM can lead to macrosomia in both the placenta and the newborn, along with additional obstetric risks, including mechanical complications during delivery [3,4]. However, macrosomia is not a proportionate overgrowth, as the placenta-to-fetus weight ratio at birth tends to shift towards higher values, indicating a possible relative functional deficit in the placenta [5,6]. Furthermore, hypoxic conditions are often observed in the fetus during late pregnancy in such cases [7], and histomorphometric analyses have shown effects on villous structure [2,8,9] and placental exovesicles [10] in DM/GDM.

In cases of fully controlled hyperglycemia, the pregnancy usually proceeds without macrosomia of either the placenta or the newborn. Therefore, clinically well-controlled GDM pregnancies do not differ substantially from the course and outcome of uncomplicated pregnancies. Though some qualitative histopathological differences in the placenta have been observed even with well-controlled GDM/DM [7,11], quantitative histomorphometric analyses using advanced first- and second-order stereology have not identified microscopic correlates for

* Corresponding author.
E-mail address: nirav.barapatre@med.uni-muenchen.de (N. Barapatre).

https://doi.org/10.1016/j.placenta.2026.01.010
Received 4 June 2025; Received in revised form 27 October 2025; Accepted 15 January 2026
Available online 16 January 2026

these qualitative findings [12]. However, stereological studies so far primarily focused on the maternal side of the placental barrier, examining star volumes and the volume of the intervillous space [12]. The intervillous space and its porosity are not more than an indirect reflection of changes in the structure of the villous tree structure, though.

We have recently introduced a novel stereology and 3D-microscopic morphometric approach that directly examines the peripheral villous tree and the villous trophoblast. This has been successfully used to analyze clinically normal placentas, placentas with fetal growth restriction, and preeclamptic placentas [13–15]. In this study, we apply the same analysis strategy to placentas affected by well-controlled GDM, with special attention to possible sex-related effects on placental structure. Our findings reveal sexual dimorphism on the villous surface, alongside sex-independent alterations of the branching patterns of the villous tree.

2. Materials and methods

2.1. Clinical groups and placental tissue

The current study used a pool of 20 placentas from clinically normal pregnancies (Control) and 20 placentas from pregnancies with GDM. Clinically, GDM was diagnosed by a pathological oral glucose tolerance test (OGTT) as defined by the guidelines. The women with GDM were treated successfully by diet or appropriate medication according to relevant German and European guidelines. The treatment was successful, as no macrosomia was recorded either of placenta or fetus. All placentas were obtained from the Department of Obstetrics and Gynecology at the "Dritter Orden" hospital in Munich, Germany. Essential clinical data and gross anatomical placental information are presented in Table 1. All methods and procedures were conducted in compliance with relevant guidelines and regulations. The ethics board of Ludwig-Maximilians-University of Munich (LMU Munich) granted approval for all investigations under the numbers 084–11 and 478–12. Placentas were collected after obtaining informed consent from the mothers/parents.

Immediately after birth, all placentas were cooled at a temperature of 4 °C and transported under continuous refrigeration to the Department of Anatomy II at LMU Munich. At the department, weight, thickness and diameters of the placentas were measured before taking whole-depth samples. Tissue sampling was carried out using a well-established systematic and random procedure [13].

2.2. Stereology

All control and GDM placentas were analyzed by Stereology by a single operator. Representative thin sections were taken from the whole-depth placental blocks and quantified by stereology as described in Ref. [14]. Briefly, immunohistochemical double staining of the perivascular sheath and the fetal villous endothelium was performed by targeting γ-sm-actin (1:900 in PBS buffer; article no. 69133; MP Biomedicals, Eschwege, Germany) and CD34 (1:900 in PBS buffer; article no. MS-363-PO; Thermo Fisher Scientific, Dreieich, Germany), respectively. Villous cross-sections showing the presence of myofibroblasts through perivascular labelling of γ-sm-actin were categorized as contractile villi (C-villi), while those without myofibroblasts were classified as non-contractile villi (NC-villi) (Fig. 1). Counting points falling within an intravillous vascular lumen were registered as a partial volume of the villous volume and inherited the property of belonging to either C-villi or NC-villi.

With the "Nearest Neighbor Workflow" of Stereo Investigator (MBF Bioscience, Williston, USA), volume fractions of γ-sm-actin positive and γsm-actin negative components of the villous trees, the intervillous space, branching index, and diffusion distance were estimated. The

Table 1
Mean values and respective standard deviations for clinical, macroscopic and Stereology parameters are given in the table. Statistically significant differences, which are independent of sex, are indicated by ^{A}. Further, * denotes a significant difference from the control value for a specific group.

Variable	GDM	Control	GDM	Control	GDM	Control
	All; n = 20	All; n = 20	female; n = 10	female; n = 10	male; n = 10	male; n = 10
Maternal Age (Years)	36.8 ± 3.1	33.9 ± 5.4	36.7 ± 2.5	32.5 ± 6.4	36.8 ± 3.8	35.2 ± 5.0
Gestational Age (weeks)	39.2 ± 1.4	39.1 ± 0.7	39.4 ± 1.5	39.3 ± 0.6	39.0 ± 1.6	38.9 ± 0.8
Birth Weight (g)	3482 ± 452	3440 ± 486	3418 ± 304	3405 ± 585	3574 ± 567	3438 ± 398
Placental Weight (g)	530 ± 114	585 ± 164	556 ± 150	597 ± 124	512 ± 114	586 ± 206
Ratio PW/BW	0.15 ± 0.03	0.17 ± 0.06	0.17 ± 0.03	0.17 ± 0.03	0.15 ± 0.02	0.17 ± 0.08
Total Villous Volume (ml)	250 ± 62	271 ± 82	271 ± 87	276 ± 84	235 ± 64	266 ± 83
Volume IVS (ml)	282 ± 60	304 ± 78	290 ± 74	304 ± 66	278 ± 56	320 ± 128
Volume Fraction IVS	52.1 ± 3.8	54.2 ± 3.8	50.7 ± 3.6	53.2 ± 5.9	53.5 ± 3.5	54.2 ± 2.3
C-villi						
Villous Volume (ml)	105 ± 35	108 ± 40	111 ± 42	112 ± 39	99 ± 32	103 ± 42
Villous Branching Index	**16.8^{A} ± 2.4**	32.9 ± 4.3	**16.2* ± 2.5**	32.3 ± 5.7	**17.3* ± 2.2**	33.5 ± 3.7
Vessel Volume (ml)	28.1 ± 11.8	26.5 ± 15.2	28.3 ± 12.9	29.2 ± 16.6	27.8 ± 11.5	23.8 ± 12.9
Vessel Branching Index	**2.5^{A} ± 1.3**	4.1 ± 2.1	2.6 ± 1.2	4.4 ± 2.3	2.3 ± 1.5	3.73 ± 2.00
Diffusion Distance (μm)	17.0 ± 2.6	17.8 ± 2.6	16.2 ± 2.4	16.5 ± 1.7	17.8 ± 2.5	19.5 ± 3.8
SD of Diffusion Distance (μm)	12.5 ± 1.6	13.1 ± 2.4	12.1 ± 1.6	13.0 ± 1.4	12.8 ± 1.6	14.6 ± 4.5
NC-villi						
Villous Volume (ml)	153 ± 45	166 ± 56	165 ± 47	163 ± 52	139 ± 45	170 ± 66
Villous Branching Index	**12.2^{A} ± 1.6**	22.2 ± 2.8	**12.6* ± 1.6**	22.2 ± 2.3	**11.8* ± 1.8**	22.0 ± 3.7
Vessel Volume (ml)	131 ± 37	141 ± 45	140 ± 36	138 ± 39	118 ± 39	145 ± 55
Vessel Branching Index	**3.6^{A} ± 1.0**	5.6 ± 1.3	**3.8* ± 1.2**	5.7 ± 1.2	**3.4* ± 0.8**	5.4 ± 1.4
Diffusion Distance (μm)	7.7 ± 1.2	8.4 ± 1.2	6.9 ± 1.4	7.8 ± 0.6	8.2 ± 0.6	9.1 ± 1.5
SD of Diffusion Distance (μm)	**5.8^{A} ± 0.7**	6.4 ± 0.8	**5.3* ± 1.0**	6.2 ± 0.6	6.0 ± 0.3	6.7 ± 1.0
Volume Ratio (C-villi/NC-villi)	0.74 ± 0.32	0.68 ± 0.16	0.68 ± 0.26	0.69 ± 0.16	0.80 ± 0.34	0.65 ± 0.19

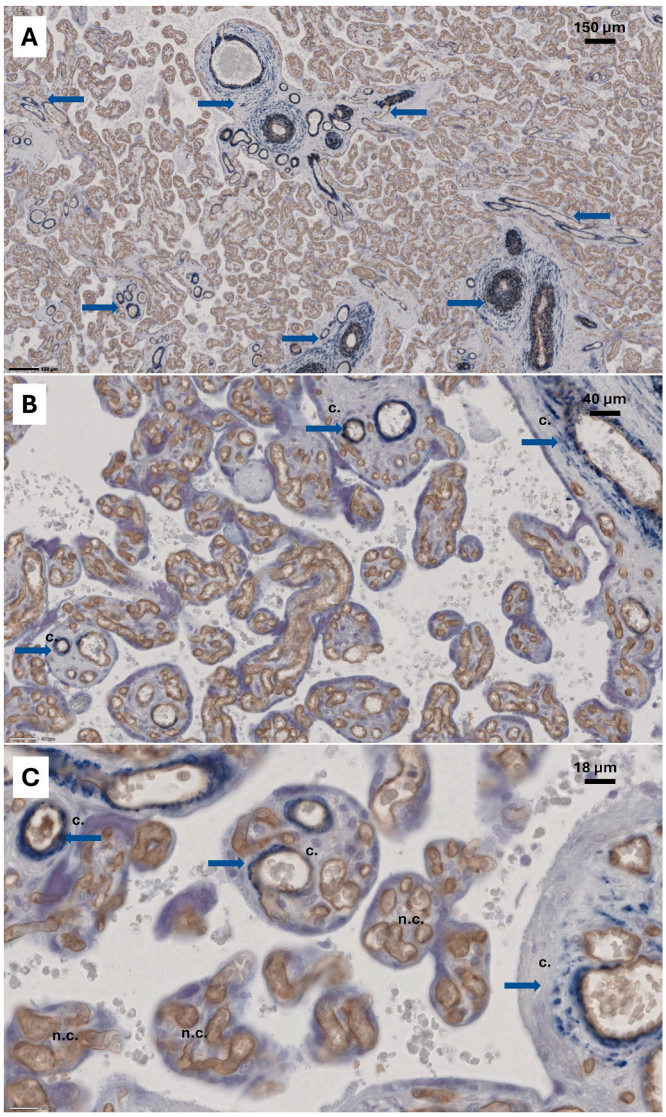

Fig. 1. IHC-guided **Stereology** (A–C) The figure shows a representative immunohistochemical double labelling of sections of villous tissue at different levels of magnification. (blue arrows) The dark blue staining is a marker of γ-sm-actin and indicates the presence of perivascular myofibroblasts and the perivascular contractile sheath of placental villi is labelled by. The brown colour indicates the detection of CD34 in fetal endothelial cells. The villous tree is thus compartmentalized and quantified in contractile and non-contractile parts based on the presence or absence of myofibroblasts. (For interpretation of the references to colour in this figure legend, the reader is referred to the Web version of this article.)

calculation of branching index has been described previously in Refs. [14,16]. Breifly, the examiner had to assess, whether the shape of the villous surface at the measurement point as being either concave or straight/convex. The ratio of concave to straight/convex villous surfaces is an indicator of branching as concave villous surfaces occur only in cross-sections through branching points. In the moderately tortuous villous tree, a high fraction of concave surface of villous cross-sections is an indicator of more branching points in the section.

2.3. 3D microscopy

All control and 11 GDM placentas (5 male, 6 female) were analyzed by 3D microscopy by a single operator. For 3D microscopy measurements, small bushes of the peripheral villous tree were isolated and processed as described in detail in Refs. [13,16]. Briefly, the villous trees were first fixed in 4.5 % formaldehyde. The proliferative nuclei were stained selectively by immunohistochemical reaction targeting proliferating cell nuclear antigen (PCNA) (mouse anti-PCNA, 1:9000 in PBS buffer; article no. 180110; Invitrogen). Non-proliferative nuclei were counterstained using hematoxylin. The isolated villous tree was then transferred on a concave slide to achieve a whole-mount preparation for tracing.

Manual tracing of all peripheral villous trees was performed using Neurolucida software (version 11.02; MBF Bioscience, Williston, VT, USA) under a brightfield microscope with a 20x objective. The tracing of at least two outermost branch generations was done in the direction from the proximal end to the terminal end of the peripheral villous tree.

The quantified data encompassed branching angles, villous diameters, lengths, villous surface area, and villous volume. Also, the number of PCNA-positive and PCNA-negative nuclei, together with their individual 3D coordinates, was registered. The data were stratified according to the branch generation.

2.4. Statistical analysis

The software R [17] was used to perform descriptive and inferential statistical analysis. Comparisons and statistical testing between the groups were performed using robust statistical methods [18,19], which compare trimmed or Winsorized means to minimize the influence of outliers. The point estimates in the forest plots are calculated as deviations of GDM means from Control means in percent. The two-tailed confidence intervals are calculated with an alpha value of 0.05 and a z-statistic of 1.96.

3. Results

3.1. Clinical and macroscopic data

The clinical and macroscopic parameters maternal age, gestational age, birth weight, placental weight and the placenta to birth weight ratio showed no significant differences between control placentas and placentas affected by GDM. Furthermore, subgroup analysis by fetal sex also reveals no significant interaction between the disease and the fetal sex (Fig. 2, Table 1).

3.2. Volumes of the villous tree

The total volume of the villous tree and the volume of the intervillous space do not differ significantly between placentas affected by GDM and control placentas, nor between placentas of different sexes, regardless of group membership (Table 1, Fig. 3).

When differentiated between the contractile (C-villi) and non-contractile (NC-villi) components of the villous tree, the volumes of C-villi, NC-villi, and the volume ratio of C-villi to NC-villi show no significant differences between placentas affected by GDM and control placentas. The difference in volumes of these parameters remained non-significant when the fetal sex was considered (Table 1, Fig. 3).

Similarly, the volumes of the vessels of the C-villi and the vessels of the NC-villi also do not differ significantly between placentas affected by gestational diabetes and normal placentas, nor between placentas of different sexes, regardless of group membership (Table 1).

3.3. Branching Index

The branching index is significantly lower in both, the C-villi and the NC-villi, regions of placentas affected by GDM compared to placentas from control pregnancies. Subanalysis by sex also reveals significantly lower branching indices in GDM, both in female and male placentas (Fig. 3, Table 1).

The branching index of vessels in C-villi is statistically significantly reduced in GDM villous trees, only when the fetal sex is not considered.

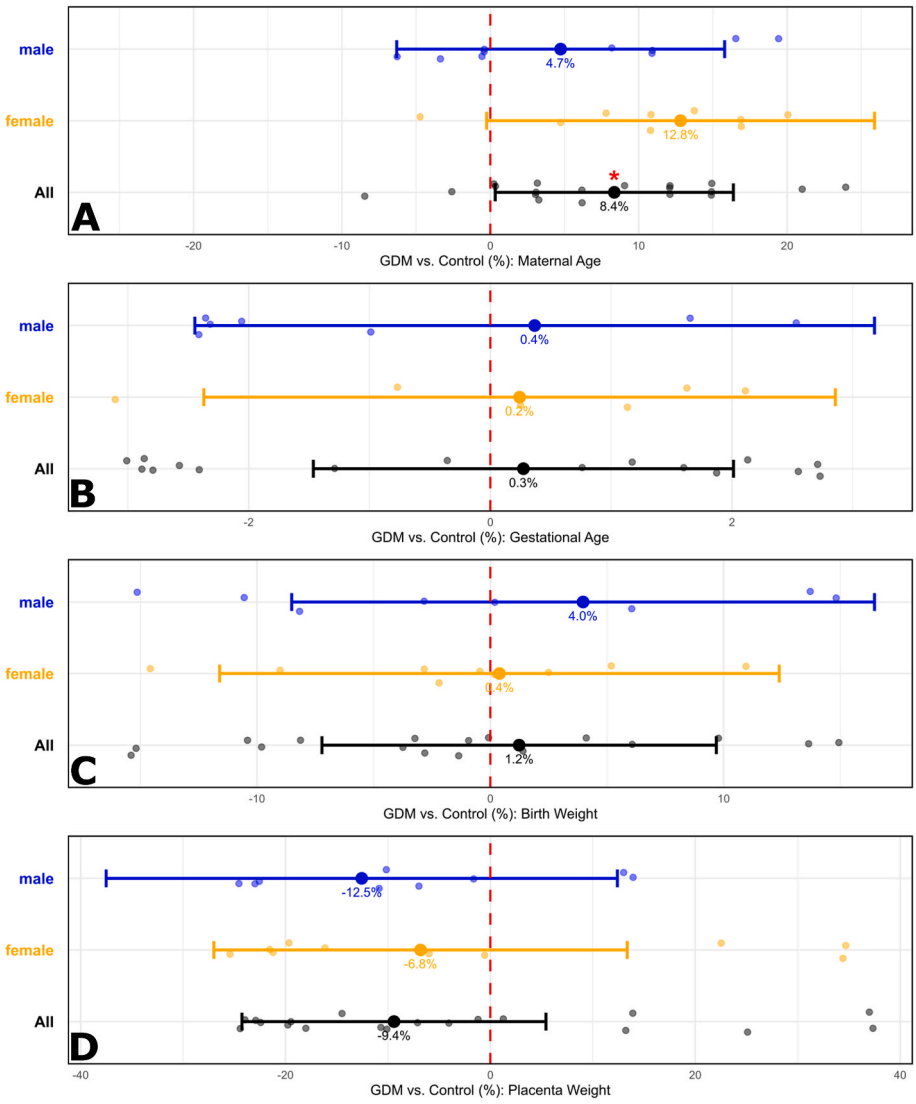

Fig. 2. Cli**nical Data** The forest plots (A–D) compare GDM data with Control data (represented by the red dashed zero line at the centre of each tile). GDM data are shown as mean values (large points) with 95 % confidence intervals (bars) as deviation from zero in percent. Individual data points are smaller and semitransparent, jittered along the confidence intervals. Black data points (All) represent all placentas, orange (female) represent female placentas only, and blue (male) represent male placentas only. Statistical significance is indicated by confidence intervals that do not intersect the zero line, marked with a red asterisk above the mean value. The figure displays data on the Maternal Age (A), Gestational Age (B), Birth Weight (C) and Placental Weight (D). (For interpretation of the references to colour in this figure legend, the reader is referred to the Web version of this article.)

In sex-specific subgroup analysis, which uses a robust but conservative approach, the differences are no longer statistically significant (Table 1). However, the 95 % confidence intervals for both, male and female, are lower than zero, indicating a significant departure from control (Fig. 3). The branching index of vessels in NC-villi is statistically significantly reduced in GDM placentas independent of fetal sex. This statement holds true for sex-specific subgroup analysis in NC-villi (Fig. 3, Table 1).

3.4. *Fetomaternal diffusion distance*

The diffusion distance between maternal and fetal circulation is not significantly different between placentas from control and GDM pregnancies, both in the overall group analysis and in the sex-specific subgroup analysis (Fig. 3, Table 1).

In the overall analysis, the standard deviation of the diffusion distance between maternal and fetal circulation in the NC-villi is lower in the GDM group compared to the Control group. This finding was statistically significant in the female subgroup but not in the male subgroup. There were no differences observed in the standard deviation of the diffusion distance for the entire group of C-villi, both in the overall analysis and in the gender-specific subgroup analysis (Table 1).

3.5. *Data from 3D microscopy*

Since only a subset of GDM placentas were analyzed by 3D Microscopy, statistically significant differences were observed in the gestational age (male GDM placentas) and the placental weight (female GDM placentas). These minor differences, however, do not influence the parameters measured by 3D microscopy.

The mean nuclear distances between PCNA-negative cell nuclei of the villous trophoblast are significantly larger in GDM placentas compared to control placentas. In subgroup analysis, this increase is significant only in female placentas, with no difference observed in male placentas (Fig. 4, Table 2).

Conversely, the mean nuclear distances between PCNA-positive cell nuclei of the villous trophoblast are significantly smaller in GDM placentas compared to control placentas. In subgroup analysis, this reduction is significant only in female placentas, with no difference

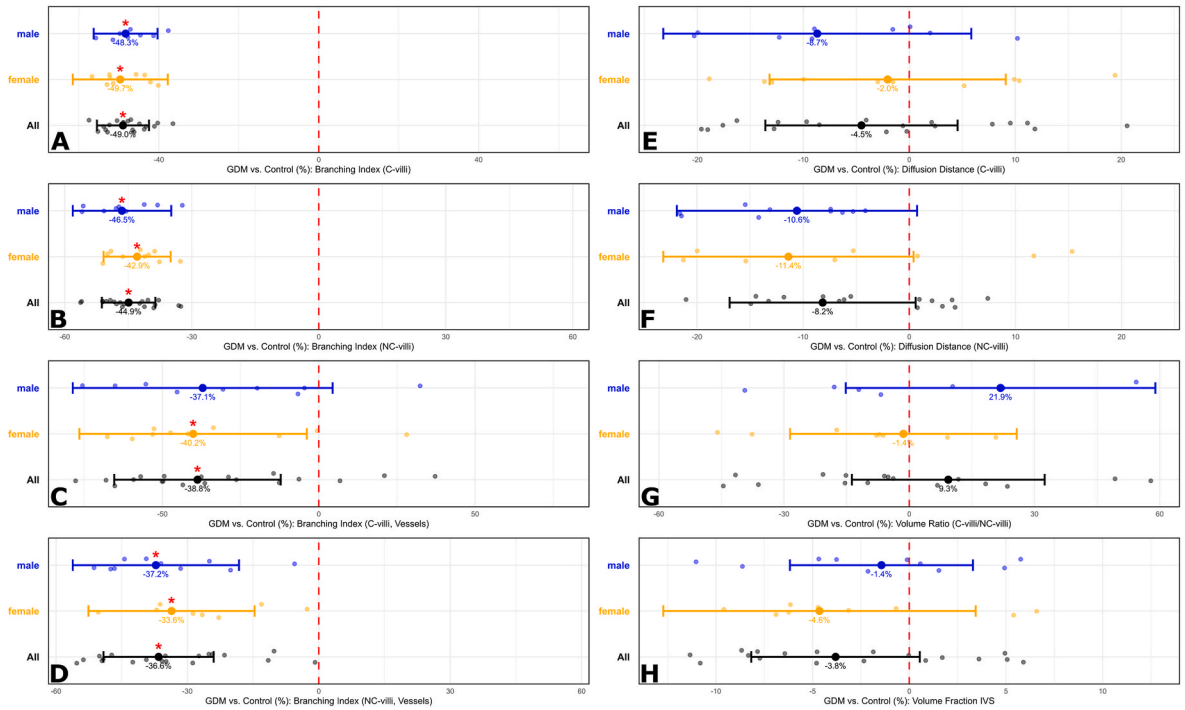

Fig. 3. Stereological Data The forest plots (A–H) compare GDM data with Control data (represented by the red dashed zero line at the centre of each tile). GDM data are shown as mean values (large points) with 95 % confidence intervals (bars) as deviation from zero in percent. Individual data points are smaller and semi-transparent, jittered along the confidence intervals. Black data points (All) represent all placentas, orange (female) represent female placentas only, and blue (male) represent male placentas only. Statistical significance is indicated by confidence intervals that do not intersect the zero line, marked with a red asterisk above the mean value. The figure displays data on the Branching Index (A–D) of C-villi (A) and NC-villi (B), as well as vessel data in the villous tree for C-villi (C) and NC-villi (D). The fetomaternal diffusion distance is shown for C-villi (E) and NC-villi (F). The ratio of C-villi to NC-villi volumes (G), and the volume fraction of the intervillous space (H), are shown as general measures of the villous tree structure. (For interpretation of the references to colour in this figure legend, the reader is referred to the Web version of this article.)

observed in male placentas (Fig. 4, Table 2).

The surface density of PCNA-negative cell nuclei of the villous trophoblast on the surfaces of villi is significantly lower in GDM placentas compared to control placentas. This holds true for both terminal branches (bT0) and pre-terminal villous branches (bT1). In gender-specific subgroup analysis, the surface density of PCNA-negative cell nuclei on the villous trophoblast surfaces is significantly reduced only in female placentas; no difference is observed in male placentas (Fig. 4, Table 2).

The surface density of PCNA-positive cell nuclei of the villous trophoblast on the terminal branches (bT0) of the villous tree is significantly higher in GDM placentas compared to control placentas. This difference is not observed in the pre-terminal branches (bT1) of the villous tree. In gender-specific subgroup analysis, the surface density of PCNA-positive cell nuclei on the villous trophoblast surfaces of GDM placentas is significantly higher only in female placentas; there is no group-related or gender-related difference observed in male placentas (Fig. 4, Table 2).

4. Discussion

The present investigation utilizes three-dimensional microscopy and stereology as complementary morphometric methodologies to assess the functional microarchitecture of the placenta. Our primary emphasis is on the structural modifications occurring within the villous trophoblast and the villous tree [13–15,20], rather than the intervillous pores [12]. Both three-dimensional microscopy and stereology revealed significant structural changes in placentas associated with well-managed GDM, in the absence of macrosomia.

In this study, the trophoblast layer is conceptualized as a specialized epithelial structure, consisting of both a proliferative compartment and a functionally mature, non-proliferative compartment [13,15]. The functional renewal and integrity of the entire layer are sustained through the proliferation of cellular trophoblasts, followed by cyto-syncytial fusion within the syncytial layer, and ultimately by shedding into the uteroplacental circulation (Fig. 5). The increased density of PCNA-positive trophoblast nuclei observed on the surface of the villous trees indicates an augmented production of trophoblast material in GDM. Furthermore, the concurrent reduction in the density of PCNA-negative trophoblast nuclei suggests that the more mature segment of the trophoblast layer is also affected. We propose that this combination of heightened proliferation and a decrease in mature nuclei is largely attributable to a shortened residence time of the trophoblast nuclei within the layer prior to being shed into the maternal circulation (Fig. 5).

During pregnancy, trophoblasts typically shed materials, including placenta-derived exosomes, into maternal blood [21]. An increased and accelerated production and shedding of trophoblast material beyond normal quantities into maternal blood can be reasonably anticipated from the findings of this study in GDM. It is well-documented that levels of placenta-derived exosomes are significantly higher in GDM than in normal pregnancies [22]. However, the levels of cell-free fetal DNA in maternal plasma do not appear to increase in GDM [23]. There remains some uncertainty regarding the levels of cell-free fetal DNA in GDM, as samples were predominantly collected during the first half of pregnancy [23]. Data concerning the latter half of pregnancy in GDM is largely lacking. In cases of preeclampsia, trophoblasts also exhibit increased proliferation alongside a decreased density of PCNA-negative trophoblast nuclei [15]. Nevertheless, the levels of cell-free fetal DNA and placenta-derived exosomes [24–26] are both reported to be elevated in preeclampsia.

Irrespective of the detection of shed material in maternal plasma, the

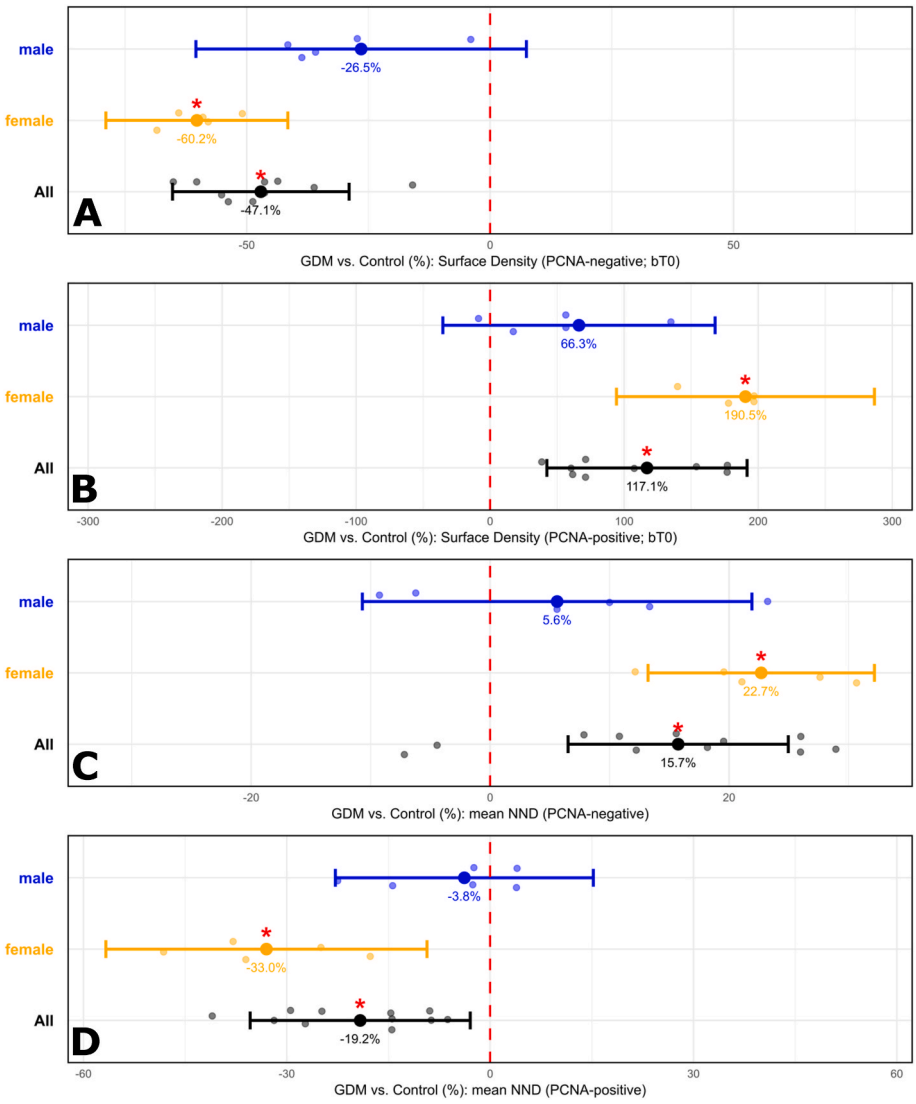

Fig. 4. Data from 3D-Microscopy The forest plots (A–D) compare GDM data with Control data (represented by the red dashed zero line at the centre of each tile). GDM data are shown as mean values (large points) with 95 % confidence intervals (bars) as deviation from zero in percent. Individual data points are smaller and semitransparent, jittered along the confidence intervals. Black data points (All) represent all placentas, orange (female) represent female placentas only, and blue (male) represent male placentas only. Statistical significance is indicated by confidence intervals that do not intersect the zero line, marked with a red asterisk above the mean value. The figure displays data on the mean Surface Density of trophoblast nuclei in the terminal branches (bT0) of the villous tree (A,B), for PCNA-negative nuclei (A) and PCNA-positive nuclei (B). C and D show the mean Nearest Neighbor Distance (NND) of PCNA-negative (C) and PCNA-positive nuclei. (For interpretation of the references to colour in this figure legend, the reader is referred to the Web version of this article.)

similarities in villous trophoblast between preeclampsia and GDM may represent a potential link between these two syndromes within the placenta, given that GDM and preeclampsia exhibit substantial comorbidity [27].

The observed sexual dimorphism in the data concerning villous trophoblast in this study is particularly noteworthy. In this investigation, the differences between groups are predominantly driven by female placentas, rather than male ones (Fig. 4). These findings closely align with those of a previous study on placentas affected by preeclampsia [15], yet contrast with results observed in fetal growth restriction, where no sexual dimorphism has been identified in villous trophoblast [13,28]. In both preeclampsia and GDM (but not in fetal growth restriction), the sexual dimorphism can be interpreted as an increase in physiological sexual dimorphism, which has also been noted in villous trophoblast [13,28]. These parallels between preeclampsia and GDM may contribute to the established comorbidity between GDM and preeclampsia [27]. The risk of developing preeclampsia is heightened in pregnancies complicated by GDM compared to those without [27]. Some studies further suggest that this comorbidity may also be influenced by fetal sex, as the risk of developing postnatal type 2 diabetes is higher for women with GDM and a female fetus than for those with GDM and a male fetus [29,30]. However, data regarding potential sexual dimorphisms related to cell-free fetal DNA in GDM are largely absent, highlighting the necessity for further studies with greater statistical power to explore associations between cell-free fetal DNA and fetal sex. The scarcity of data on the sexual dimorphism of cell-free fetal DNA partly arises from the frequent use of Y-chromosomal loci to identify the fetal origin of cell-free DNA in maternal plasma [31–33].

The present study also investigated the branching patterns of the villous trees using second-order stereology to ascertain the branching index, an established approach to villous branching [13,14]. The branching index was found to be statistically significantly lower in GDM placentas compared to controls, in both C-villi and NC-villi. This observation was not noted in the previous study on preeclampsia [15], but it does draw parallels to findings from another study on fetal growth restriction [14]. The reduction in branching is not sex-dependent and is

Table 2
Mean values and respective standard deviations for clinical, macroscopic and 3D Microscopy parameters are given in the table. Statistically significant differences, which are independent of sex, are indicated by [A]. Further, * denotes a significant difference from the control value for a specific group. The GDM samples are a subset of the samples presented in Table 1, whereas the Control samples are identical.

Variable	GDM	Control	GDM	Control	GDM	Control
	All; n = 11	All; n = 20	female; n = 5	female; n = 10	male; n = 6	male; n = 10
Maternal Age (Years)	36.3 ± 3.3	33.9 ± 5.4	37.0 ± 2.1	32.5 ± 6.4	35.8 ± 3.7	35.2 ± 5.0
Gestational Age (weeks)	**40.1[A] ± 1.0**	39.1 ± 0.7	40.4 ± 0.9	39.3 ± 0.6	**39.9* ± 1.3**	38.9 ± 0.8
Birth Weight (g)	3625 ± 518	3440 ± 486	3440 ± 336	3405 ± 584	3765 ± 578	3438 ± 398
Placental Weight (g)	521 ± 137	585 ± 164	**473* ± 25**	597 ± 124	556 ± 149	586 ± 206
Ratio PW/BW	0.15 ± 0.02	0.17 ± 0.04	0.15 ± 0.02	0.17 ± 0.04	0.15 ± 0.02	0.17 ± 0.08
PCNA-negative nuclei						
Mean NND (μm)	**6.7[A] ± 0.7**	5.8 ± 0.8	**7.0* ± 0.5**	5.7 ± 0.5	6.2 ± 1.0	5.9 ± 0.9
Surface Density bT0 (10-3μm-2)	**4.23[A] ± 1.18**	7.99 ± 2.90	**3.48* ± 0.71**	8.77 ± 2.45	5.16 ± 1.69	7.02 ± 3.16
Surface Density bT1 (10-3μm-2)	**4.08[A] ± 2.15**	7.26 ± 3.23	**3.18* ± 0.88**	8.03 ± 3.00	4.75 ± 2.09	6.08 ± 4.58
PCNA-positive nuclei						
Mean NND	**12.5[A] ± 2.1**	15.5 ± 5.0	**11.8* ± 2.8**	17.6 ± 5.5	13.0 ± 1.6	13.6 ± 3.6
Surface Density bT0 (10-3μm-2)	**0.94[A] ± 0.37**	0.43 ± 0.54	**0.73* ± 0.12**	0.25 ± 0.35	1.28 ± 0.68	0.77 ± 0.91
Surface Density bT1 (10-3μm-2)	0.80 ± 0.49	0.57 ± 0.65	1.10 ± 0.69	0.30 ± 0.23	0.70 ± 0.37	0.88 ± 0.78

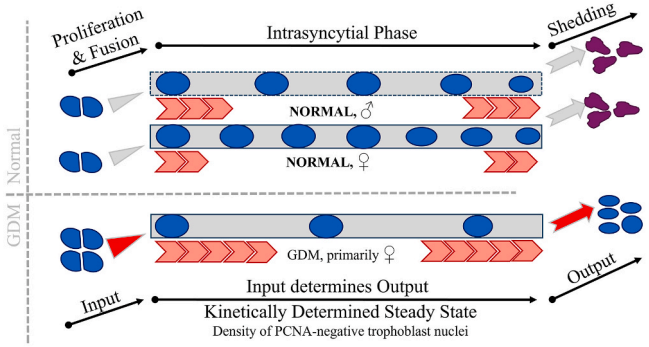

Fig. 5. The figure shows a schematic representation of the passage of trophoblast nuclei in control (top) and GDM (bottom) placentas. The blue circles represent the trophoblast nuclei, which proliferate (left) and fuse with the syncytium (center) before being shed (right) in the maternal circulation. The red arrows indicate qualitatively the speed of transition through the intrasyncytial phase. maternal circulation. The red arrows indicate the speed of transition through the intrasyncytial phase. (For interpretation of the references to colour in this figure legend, the reader is referred to the Web version of this article.)

remarkably clear for a morphometric method in placental research, with no overlap in standard deviations and minuscule p-values in the statistical tests. The absence of differences in caliber or volume of the villi could be attributed to the missing placental macrosomia in GDM. The reduced branching, however, is present even in the absence of placental or fetal macrosomia. The presence of these changes in both C-villi and NC-villi suggests that the disruption in branching may commence early in pregnancy and persist. While most NC-villi are situated in the terminal regions of the villous tree, having formed primarily during the 3rd trimester phase of pregnancy, many C-villi are stem villi that began forming as immature intermediate villi in the first trimester [1,34]. The potential mechanisms behind this change in branching patterns and its functional implications remain unclear, though. Nevertheless, there are hints of possible discrete functional deficits in late pregnancy associated with GDM. The occurrence of fetal hypoxia in late pregnancy could imply an associated deficit in gas exchange [7,35]. Currently, it is believed that villous tree branching is driven by villous angiogenesis, with branching angiogenesis occurring in the first half of pregnancy and non-branching angiogenesis during the second half, particularly in the final trimester. However, in the GDM placentas analyzed in this study, both phases of villous branching appear to be equally influenced by the pathophysiological mechanisms of GDM. This is a remarkable finding and, at present, cannot be easily elucidated. Similarly, the branching indices of the vessels inside the C- and NC-villi, which may or may not be sex-dependent, can be thought as linked to the angiogenetic processes.

The strengths of this study lie in its focus on the structure of the villous tree. Neither trophoblast assessment at the villous surface (via three-dimensional microscopy) nor branching analysis using second-order stereology (branching index) has previously been conducted on placentas affected by GDM. The absence of observed differences in earlier studies on well-controlled GDM cases may be attributed to their focus on intervillous pores, which are only indirectly influenced by the villous tree. The limitations of the current study arise from ethical restrictions, which precluded the inclusion of more detailed clinical records in the evaluation. Future studies, incorporating more extensive clinical data, could address these limitations.

5. Conclusion

No differences in the clinical parameters like gestational age, birth weight, and placental weight suggest that the GDM pregnancies were well-managed. The GDM placentas, however, show a markedly pronounced reduction in the branching index across both sexes. The villous trophoblast, on the other hand, shows a sexually dimorphic alteration in the density of proliferative and non-proliferative nuclei. This finding is similar to the observation made in preeclamptic placentas.

CRediT authorship contribution statement

N. Barapatre: Writing – review & editing, Writing – original draft, Visualization, Supervision, Project administration, Methodology, Investigation, Funding acquisition, Formal analysis, Conceptualization. **L. Halm:** Investigation, Formal analysis, Data curation. **C. Schmitz:** Supervision, Methodology. **F.E. von Koch:** Supervision, Methodology, Formal analysis, Conceptualization. **C. Kampfer:** Formal analysis. **H-G. Frank:** Writing – review & editing, Writing – original draft, Visualization, Supervision, Project administration, Methodology, Investigation, Funding acquisition, Formal analysis, Conceptualization.

Declaration of competing interest

None.

Acknowledgements

The authors acknowledge skillful technical assistance and diligent work of technicians of the Department of Anatomy II at LMU Munich, namely B. Aschauer and A. Baltruschat. Funding was provided by the Deutsche Forschungsgemeinschaft (Fr1245/9-2 to HGF; BA 3896/2-2 to NB).

References

[1] R.N. Baergen (Ed.), Benirschke's Pathology of the Human Placenta, seventh ed., Springer International Publishing AG, Cham, 2022 https://doi.org/10.1007/978-3-030-84725-8.
[2] J. Huynh, D. Dawson, D. Roberts, R. Bentley-Lewis, A systematic review of placental pathology in maternal diabetes mellitus, Placenta 36 (2015) 101–114.
[3] B.E. Metzger, L.P. Lowe, A.R. Dyer, E.R. Trimble, U. Chaovarindr, D.R. Coustan, D. R. Hadden, D.R. McCance, M. Hod, H.D. McIntyre, J.J.N. Oats, B. Persson, M. S. Rogers, D.A. Sacks, Hyperglycemia and adverse pregnancy outcomes, N. Engl. J. Med. 358 (2008) 1991–2002.
[4] K. Kc, S. Shakya, H. Zhang, Gestational diabetes mellitus and macrosomia: a literature review, Ann. Nutr. Metabol. 66 (Suppl 2) (2015) 14–20.
[5] C. Bianchi, E. Taricco, M. Cardellicchio, C. Mandò, M. Massari, V. Savasi, I. Cetin, The role of obesity and gestational diabetes on placental size and fetal oxygenation, Placenta 103 (2021) 59–63.
[6] E. Taricco, T. Radaelli, M.S. Nobile de Santis, I. Cetin, Foetal and placental weights in relation to maternal characteristics in gestational diabetes, Placenta 24 (2003) 343–347.
[7] G. Daskalakis, S. Marinopoulos, V. Krielesi, A. Papapanagiotou, N. Papantoniou, S. Mesogitis, A. Antsaklis, Placental pathology in women with gestational diabetes, Acta Obstet. Gynecol. Scand. 87 (2008) 403–407.
[8] E. Jauniaux, G.J. Burton, Villous histomorphometry and placental bed biopsy investigation in type i diabetic pregnancies, Placenta 27 (2006) 468–474.
[9] F. Teasdale, Histomorphometry of the human placenta in class b diabetes mellitus, Placenta 4 (1983) 1–12.
[10] X. Liu, H. Qiu, Placenta-derived exosomes and gestational diabetes mellitus, Diabetes, Metab. Syndrome Obes. Targets Ther. 15 (2022) 1391–1404.
[11] P.A. Boyd, A. Scott, J.W. Keeling, Quantitative structural studies on placentas from pregnancies complicated by diabetes mellitus, Br. J. Obstet. Gynaecol. 93 (1986) 31–35.
[12] T.M. Mayhew, I.C. Jairam, Stereological comparison of 3d spatial relationships involving villi and intervillous pores in human placentas from control and diabetic pregnancies, J. Anat. 197 (Pt 2) (2000) 263–274.
[13] N. Barapatre, E. Haeussner, D. Grynspan, C. Schmitz, F. Edler von Koch, H.-G. Frank, The density of cell nuclei at the materno-fetal exchange barrier is sexually dimorphic in normal placentas, but not in IUGR, Sci. Rep. 9 (2019) 2359.
[14] N. Barapatre, C. Kampfer, S. Henschen, C. Schmitz, F. Edler von Koch, H.-G. Frank, Growth restricted placentas show severely reduced volume of villous components with perivascular myofibroblasts, Placenta 109 (2021) 19–27.
[15] N. Barapatre, L. Hansen, C. Kampfer, T. Rübelmann, C. Schmitz, F. von Koch, H. Frank, Trophoblast proliferation is higher in female than in male preeclamptic placentas, Placenta 158 (2024) 310–317.
[16] N. Barapatre, H.-G. Frank, Three-dimensional microarchitecture of the human placental villous tree in health and disease, Front. Cell Dev. Biol. 13 (2025) 1639740.
[17] R Core Team, R, A Language and Environment for Statistical Computing, R Foundation for Statistical Computing, Vienna, Austria, 2021. URL: https://www.R-project.org/.
[18] P. Mair, R. Wilcox, Robust statistical methods in r using the wrs2 package, Behav. Res. Methods 52 (2020).
[19] I. Patil, Visualizations with statistical details: the 'ggstatsplot' approach, J. Open Source Softw. 6 (2021) 3167.
[20] A. Buehlmeyer, N. Barapatre, C. Schmitz, F. Edler von Koch, E. Haeussner, H.-G. Frank, The volume of villi with γ-sm-actin positive perivascular cells correlates with placental weight and thickness, Placenta 85 (2019) 24–31.
[21] S. Sarker, K. Scholz-Romero, A. Perez, S.E. Illanes, M.D. Mitchell, G.E. Rice, C. Salomon, Placenta-derived exosomes continuously increase in maternal circulation over the first trimester of pregnancy, J. Transl. Med. 12 (2014) 204.
[22] C. Salomon, K. Scholz-Romero, S. Sarker, E. Sweeney, M. Kobayashi, P. Correa, S. Longo, G. Duncombe, M.D. Mitchell, G.E. Rice, S.E. Illanes, Gestational diabetes mellitus is associated with changes in the concentration and bioactivity of placenta-derived exosomes in maternal circulation across gestation, Diabetes 65 (2016) 598–609.
[23] M.K. Hopkins, N. Koelper, W. Bender, C. Durnwald, M. Sammel, L. Dugoff, Association between cell-free dna fetal fraction and gestational diabetes, Prenat. Diagn. 40 (2020) 724–727.
[24] K.D. Gerson, S. Truong, M.J. Haviland, B.M. O'Brien, M.R. Hacker, M.H. Spiel, Low fetal fraction of cell-free dna predicts placental dysfunction and hypertensive disease in pregnancy, Pregnancy Hypertens. 16 (2019) 148–153.
[25] E. Contro, D. Bernabini, A. Farina, Cell-free fetal dna for the prediction of pre-eclampsia at the first and second trimesters: a systematic review and meta-analysis, Mol. Diagn. Ther. 21 (2017) 125–135.
[26] A. Karapetian, O. Baev, A. Sadekova, A. Krasnyi, G. Sukhikh, Cell-free foetal dna as a useful marker for preeclampsia prediction, Reproductive sciences (Thousand Oaks, Calif.) 28 (2021) 1563–1569.
[27] Y. Yang, N. Wu, Gestational diabetes mellitus and preeclampsia: correlation and influencing factors, Front. Cardiovasc. Med. 9 (2022).
[28] E. Haeussner, C. Schmitz, D. Grynspan, F. Edler von Koch, H.-G. Frank, Syncytial nuclei accumulate at the villous surface in iugr while proliferation is unchanged, Placenta (2017) 47–53.
[29] M. Al-Qaraghouli, Y.M.V. Fang, Effect of fetal sex on maternal and obstetric outcomes, Front. Pediatr. 5 (2017) 144.
[30] R. Retnakaran, B.R. Shah, Sex of the baby and future maternal risk of type 2 diabetes in women who had gestational diabetes, Diabet. Med. 33 (2016) 956–960.
[31] B. Jensen, B. Atkinson, K. Worley, Noninvasive prenatal screening and ultrasonography scan of fetal sex result discordance, J. Case Rep. Imag. Obstet. Gynecol. 8 (2022) 1–4.
[32] Y.M. Lo, N. Corbetta, P.F. Chamberlain, V. Rai, I.L. Sargent, C.W. Redman, J. S. Wainscoat, Presence of fetal dna in maternal plasma and serum, Lancet 350 (1997) 485–487.
[33] M.F. Greene, E.G. Phimister, Screening for trisomies in circulating dna, N. Engl. J. Med. 370 (2014) 874–875.
[34] H.-G. Frank, Placental development, in: R.A. Polin, S.H. Abman, D.H. Rowitch, W. E. Benitz, W.W. Fox (Eds.), Fetal and Neonatal Physiology, ume 1, Elsevier, Philadelphia, 2016, pp. 101–113.
[35] J.A. Widness, J.B. Susa, J.F. Garcia, D.B. Singer, P. Sehgal, W. Oh, R. Schwartz, H. C. Schwartz, Increased erythropoiesis and elevated erythropoietin in infants born to diabetic mothers and in hyperinsulinemic rhesus fetuses, J. Clin. Investig. 67 (1981) 637–642.